HAL
open science

Frequency and fluid effects on elastic properties of basalt: Experimental investigations

M. Adelinet, Jérôme Fortin, Y. Guéguen, A. Schubnel, Laurent Geoffroy

To cite this version:

M. Adelinet, Jérôme Fortin, Y. Guéguen, A. Schubnel, Laurent Geoffroy. Frequency and fluid effects on elastic properties of basalt: Experimental investigations. Geophysical Research Letters, 2010, 37 (2), pp.10.1029/2009GL041660. 10.1029/2009GL041660 . hal-00488505

HAL Id: hal-00488505

https://hal.science/hal-00488505v1

Submitted on 8 Jul 2021

HAL is a multi-disciplinary open access archive for the deposit and dissemination of scientific research documents, whether they are published or not. The documents may come from teaching and research institutions in France or abroad, or from public or private research centers.

L'archive ouverte pluridisciplinaire **HAL**, est destinée au dépôt et à la diffusion de documents scientifiques de niveau recherche, publiés ou non, émanant des établissements d'enseignement et de recherche français ou étrangers, des laboratoires publics ou privés.

Copyright

GEOPHYSICAL RESEARCH LETTERS, VOL. 37, L02303, doi:10.1029/2009GL041660, 2010

Click Here for Full Article

Frequency and fluid effects on elastic properties of basalt: Experimental investigations

M. Adelinet,[1,2] J. Fortin,[1] Y. Guéguen,[1] A. Schubnel,[1] and L. Geoffroy[2]

Received 4 November 2009; revised 18 December 2009; accepted 23 December 2009; published 27 January 2010.

[1] In order to investigate the effects of fluid and frequency on the elastic properties, we performed hydrostatic experiments on an Icelandic basalt specimen under both dry and saturated conditions. This basalt is characterized by a bimodal porosity, i.e., cracks and equant pores. The elastic properties -bulk moduli in our case- were investigated under high pressure through two experimental methods: (1) a classical one using ultrasonic P- and S-waves velocities (frequency 10^6 Hz), (2) and a new one, using oscillation tests (frequency 10^{-2} Hz). In dry condition, experimental data show no significant difference between high (HF) and low (LF) frequency bulk moduli. However, in saturated conditions, two effects are highlighted: a physico-chemical effect emphasized by a difference between drained and dry moduli, and a squirt-flow effect evidenced by a difference between HF and LF undrained moduli. **Citation:** Adelinet, M., J. Fortin, Y. Guéguen, A. Schubnel, and L. Geoffroy (2010), Frequency and fluid effects on elastic properties of basalt: Experimental investigations, *Geophys. Res. Lett.*, *37*, L02303, doi:10.1029/2009GL041660.

1. Introduction

[2] In the laboratory, the responses of the rock elastic velocities to stress changes in saturated or dry specimens have been studied extensively in the past using ultrasonic signals in the megahertz frequency range [*Nur and Simmons*, 1969; *Guéguen and Schubnel*, 2003; *Stanchits et al.*, 2006; *Schubnel et al.*, 2006]. However when seismic wave velocities are involved, a direct extrapolation from laboratory to field scale is not straightforward. Laboratory data are indeed obtained in the ultrasonic range, whereas field data from seismological methods are obtained at much lower frequencies (Hz). The interpretation of the seismic wave velocities, measured at the field scale, in terms of fluids and/or in terms of physical properties of the rock formation is complex [*Wang et al.*, 1990].

[3] From a theoretical point of view, when cracks or pores are connected, stress can induce fluid flow from one inclusion to an another, this is the squirt-flow effect [*O'Connell and Budiansky*, 1974; *Mavko and Nur*, 1975]. In saturated samples, several authors [*Wang and Nur*, 1990; *Schubnel and Guéguen*, 2003] have shown that the measured HF velocities are generally faster than those predicted by the equations of *Gassmann* [1951], which correspond to the LF limit of Biot's theory [*Biot*, 1956].

[4] Low frequency laboratory data exist however. One technique to measure low frequency elastic moduli is to record stress-strain behavior of the rock, using axial low amplitude deformation [*Batzle et al.*, 2006; *Adam et al.*, 2006; *Adam and Batzle*, 2008]. In this study we report HF data (ultrasonic) together with LF data obtained through a new technique, also based on stress-strain behavior, but using volumetric deformation. This new technique allow us to investigate the effect of frequency dependence on the elastic properties (bulk modulus) of a basalt rock. Measurements have been performed in the pressure range of 0–200 MPa, both for low frequency (0.01–0.1 Hz) and high frequency (1 MHz).

2. Sample Description and Experimental Set-Up

[5] Iceland is an offshore part of the mid-Atlantic spreading ridge. It is an ideal laboratory to study the interplay between fluids and tectonics at oceanic ridges [*Geoffroy and Dorbath*, 2008]. A block of basalt was extracted on a road outcrop in the Reykjanes Peninsula during summer 2007. The investigated basalt (ISL 26) is fresh and young (less than 10000 years [*Sigurdsson et al.*, 2000]). Note that it is an alkali basalt containing mm-sized phenocrysts of pyroxene and microliths of feldspar. Cylindrical samples were cored in the block with a diameter of 40 mm and 80 mm in length. The samples have a water permeability of 10^{-15} m^2. Data on open porosity, pore size distribution and bulk density were obtained in a mercury porosimeter, on an Autopore IV 9500 Micromeritics. The entrance pore radius is directly derived from the intrusion mercury pressure by the Washburn law. The open porosity is 7.93%, the bulk density is 2.77 (3.00 for skeletal density) and the average pore diameter is 0.19 μm. The pore distribution is clearly bimodal (Figure 1). One peak is around 0.1 μm and an other one around 100 μm. They can be related to two types of porosity: cracks and equant pores. SEM micrographs confirm this interpretation (Figure 1). Moreover cracks and equant porosity represent respectively about 1% and 7%.

[6] The experiments were conducted on a triaxial cell installed in the Laboratoire de Géologie at the École Normale Supérieure [*Fortin et al.*, 2005]. We conducted one hydrostatic experiment in two cycles, at room temperature. The basalt sample is dinitrogen saturated in the first cycle and water saturated in the second cycle. In both cycles, the confining pressure, P_c, is increased from 10 to 200 MPa. The pore pressure is fixed to 10 MPa. *Dunn* [1987] shown that open boundaries in the pore-fluid system can cause a fluid flow effect leading to an artificial dispersion. Our sample is jacketed to isolate it from the oil confining pressure, lateral fluid flow is prevented. Only fluid movement within the small pore fluid duct can affect

[1]Laboratoire de Géologie, UMR 8538, ENS, CNRS, Paris, France.
[2]LGRMP, UMR 6112, Université du Maine, CNRS, Le Mans, France.

Copyright 2010 by the American Geophysical Union.
0094-8276/10/2009GL041660$05.00

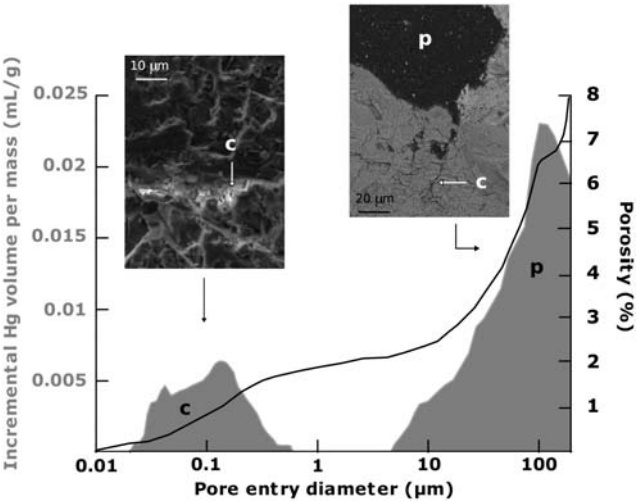

Figure 1. Mercury Intrusion Porosimetry data associated to electronic microscopy pictures. Here *p* stands for spherical pore, and *c* stands for crack. Cracks and pores porosity are about 1% and 7%, respectively. The total porosity is 8%.

the data. This effect should be small and should not be dependent on the confining pressure.

[7] Two pairs of strain gauges, glued directly on the sample, measure the axial, ε_a and radial strain, ε_r. From this, the volumetric strain ε_v is deduced as: $\varepsilon_v = \varepsilon_a + 2\varepsilon_r$. Strain measurement accuracy is close to 10^{-6}. The LF bulk modulus is measured by oscillating the confining pressure and measuring the resulting volumetric strain (Figure 2). For $P_c \leq 100$ MPa, the bulk modulus has been measured at frequencies $f = 0.01$ *Hz*, $f = 0.05$ *Hz* and $f = 0.1$ *Hz*. For $P_c > 100$ *MPa*, the bulk moduli has been measured at $f = 0.01$ *Hz*. As no difference was observed in this range of frequencies, the data presented in this paper are the ones obtained at 0.01 Hz only; the error bar is directly calculated from the regression coefficient (Figure 2). The uncertainty of LF measurements increases for $P_c > 100$ *MPa*, this can be partially explained by the experimental set-up: for $P_c \leq 100$ *MPa* the confining pressure is given by an hydraulic pump, but for $P_c > 100$ *MPa* we used an intensifier (which multiplies the pressure by 3).

[8] At ultrasonic frequencies (1 MHz), we measured the time of flight of a pulse transmitted through the rock sample, using piezoceramics (PZT). From the determination of P and S waves arrivals, P and S waves velocities are obtained and from these the rock HF elastic moduli. These moduli are considered as adiabatic ones. However LF moduli are not strictly adiabatic. And yet the dispersion due to adiabatic-isothermal transition in our case can be estimated to less than 1%.

3. Results

[9] Figure 3 summarizes the mechanical data. From strain data, we get porosity (Figures 3a–3b). In dry condition, porosity decreased during loading, from 7.93% at ambient pressure to 6.95% at 190 MPa pressure. A similar trend is observed in saturated conditions (Figure 3b). In both cases, the reduction of porosity is about 1%, a value which corresponds to the initial crack porosity (Figure 1). During the loading phases, the elastic waves velocities increased (Figure 3c–3d): respectively by 30% and 20% for P-waves and by 25% and 20% for S-waves. P - and S -waves velocities reached maximum values close to 5.2 km/s and 3.1 km/s at 190 MPa effective pressure in saturated conditions.

[10] Using the effective medium model presented by *Fortin and Guéguen* [2007], P and S waves data can be inverted to estimate a crack density ρ_c. Figure 3e–3f gives the results and shows that crack density decreases from 0.6 to 0.1 when confining pressure is increased from 0 to 100 MPa. In the saturated case, the evolution of the crack aspect ratio ξ can also be derived from the velocities evolution (Figure 3f). This parameter increases with load-

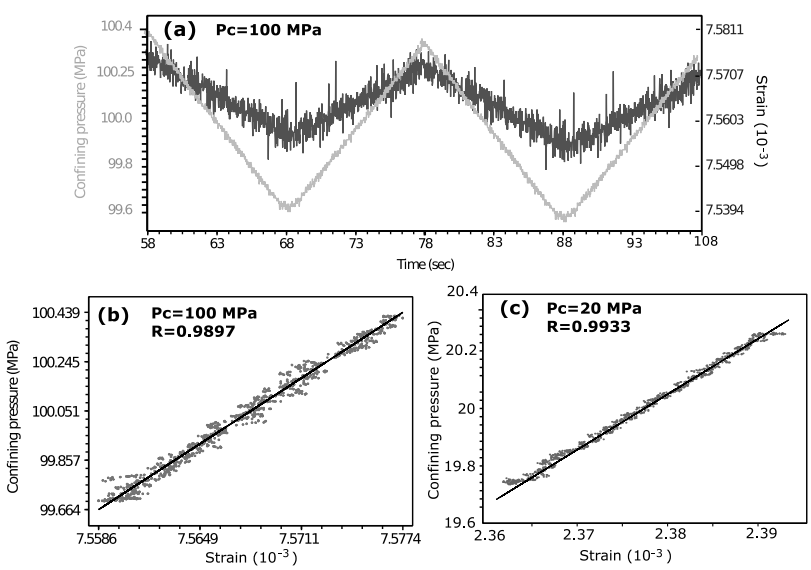

Figure 2. Oscillation tests: (a) confining pressure P_c and strain versus time over two periods for $P_c = 100$ *MPa* and confining pressure versus strain for (b) $P_c = 100$ *MPa* and (c) $P_c = 20$ *MPa*.

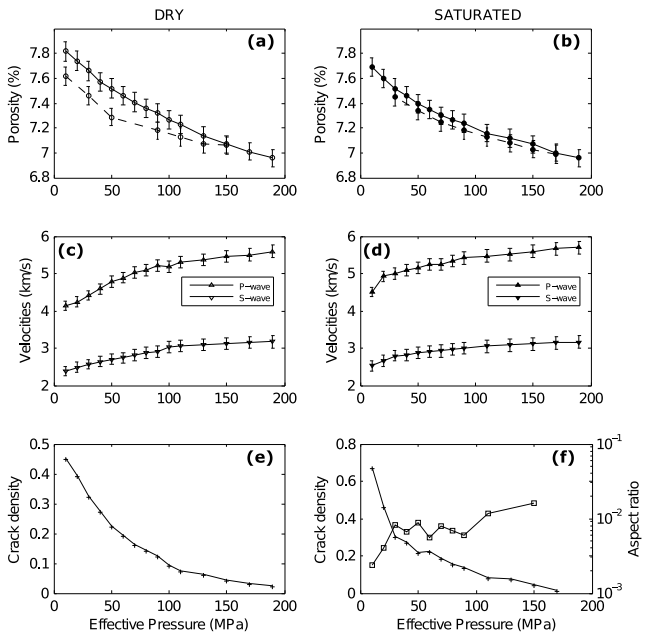

Figure 3. Mechanical data, elastic waves velocities, and effective medium inversion data for the triaxial experiment performed on ISL 26. The data are obtained in (left) dry and (right) saturated conditions, respectively. (a–b) Porosity evolution, where unloading is indicated as a dashed-line. (c–d) P and S wave velocities (HF). (e–f) Inverted parameters from the effective medium model used by *Fortin and Guéguen* [2007]: crack density in dry and saturated conditions and aspect ratio in saturated conditions.

ing, and is close to 10^{-2} in the range of 50 –190 MPa effective pressure, a value in a good agreement with the existing literature [*Tsuji and Iturrino*, 2008; *Schubnel et al.*, 2006]. Using the values of ρ_c and ξ at 10 MPa, the crack porosity can be estimated as $\Phi_{cr} = 2\pi\ \rho_c\ \xi = 0.97\%$, a value which is also consistent with the mercury intrusion porosimetry data and the porosity evolution during loading.

[11] The HF effective bulk moduli are directly calculated from the elastic waves velocities. Figure 4 gives the evolution of HF bulk moduli as well as LF bulk moduli with loading. With increasing confining pressure, HF and LF bulk moduli increased respectively by approximately 55% and 60% in dry conditions and by 25% and 75% in saturated conditions. Note that, HF moduli are always greater than LF moduli in agreement with previous studies [*Batzle et al.*, 2006; *Bala and Cichy*, 2007; *Adam and Batzle*, 2008]. Note also a systematic small difference between dry HF and LF moduli. This small difference can reflect a systematic bias in the different experimental methods or reflect some heterogeneities in the sample.

4. Discussion

[12] The goal of our study is to relate laboratory data to field data accounting for frequency and fluid effects. In the ultrasonic range, and because of the high compliance of cracks, fluid pressure is higher in cracks than in equant pores, the state is not isobaric and the moduli are "unrelaxed" moduli. In the low frequency range, local fluid flow takes place so that pores and cracks are isobaric and the moduli are "relaxed" ones. In the case of a cracked medium, this creates a frequency effect that can be very large and depends on crack geometry and distribution [*Le Ravalec and Guéguen*, 1996]. If cracks are randomly distributed in orientation, the frequency effect is not visible on bulk modulus but appears on shear modulus [*Endres and Knight*, 1997]. In the general case where pores and cracks are present, local fluid flow (squirt-flow) could take place: (1) between pores, (2) between cracks and (3) between pores and cracks. Case 1 is expected to result in a very small effect due to the small compliance of round pores. Case 2 is expected to result mainly in a shear modulus effect [*Le Ravalec and Guéguen*, 1996]. Case 3 is expected to result in both a shear and a bulk effect. In our case, the rock is characterized by a bimodal porosity and data shows that variations in the HF and LF bulk moduli are significant at moderate effective pressures (<130 MPa) where cracks are open. These results are consistent with a squirt-flow from cracks to pores.

[13] In LF conditions, fluid pressure has time to reach local equilibrium so that any representative elementary volume (REV) is isobaric. Then poroelastic theory applies. Elastic moduli are "relaxed" ones. Two distinct relaxed bulk moduli exist: the drained and undrained ones. Following *Cleary* [1978] three relaxation times τ can be considered when a fluid phase is saturating small scale sites: (1) τ_1 at the site scale, (2) τ_2 between sites at the REV scale (local) and (3) τ_3 between REVs at the global scale L. The third one allows to separate drained and undrained regimes. Then the time constant is $\tau_3 = \frac{L^2}{4c}$ with $c \approx \frac{\kappa}{\eta} K_0$, where κ is the permeability (m^2), K_0 is the solid bulk modulus (Pa) and η is the fluid viscosity ($Pa.s^{-1}$). For our basaltic sample

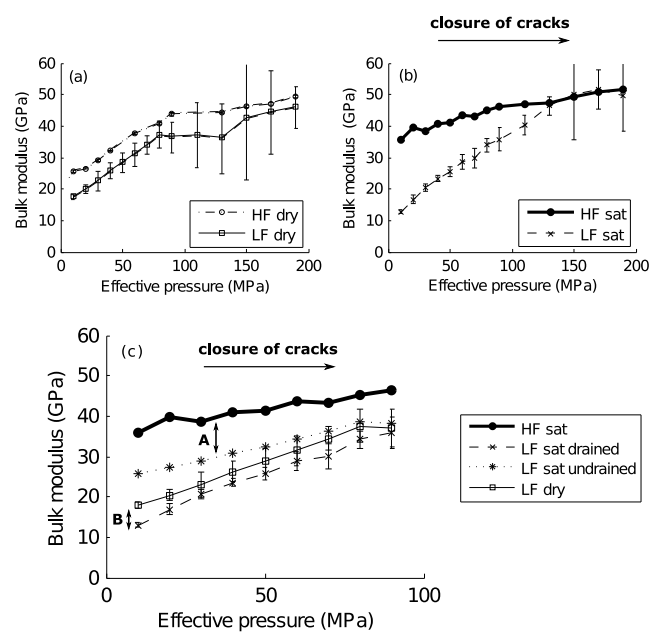

Figure 4. Bulk modulus obtained from HF velocities inversion and LF oscillation tests, 'sat' stands for saturated conditions. (a–b) All experimental results over the 0–190 MPa range. (c) The 0–100 MPa interval and also infers undrained moduli. Two effects are highlighted: A, the frequency effect, and B, the physico-chemical effect.

saturated with water, $\kappa = 10^{-15}\ m^2$, $K_0 \approx 4.10^{10}\ Pa$, $\eta = 10^{-3}\ Pa.s^{-1}$ and $L = 0.08\ m$. It results that $\tau_3 \approx 0.04\ s$. In our experiment, the frequency for LF measurements is 0.01 Hz, a value smaller than 25 Hz and also smaller than Biot cutoff frequency which can be estimated to 4 kHz. This implies that our LF bulk moduli are drained moduli. The LF undrained moduli K_u can be calculated from the LF drained moduli K_d, using Biot-Gassmann equations [*Gassmann*, 1951]. The difference is $K_u - K_d = \frac{b^2 K_f}{\Phi + (b-\Phi)\frac{K_f}{K_0}}$ where K_f is the fluid bulk modulus, Φ the porosity and b a dimensionless coefficient defined by $b = 1 - \frac{K_d}{K_0}$.

5. Conclusion

[14] Figure 4c summarizes our experimental data (HF saturated, LF dry and LF drained moduli) and the calculated ones (LF undrained moduli). Two main results can be emphasized from Figure 4c. First, it appears that the LF undrained modulus is lower than the HF saturated modulus. This implies that a frequency effect exists. This effect has been interpreted as a squirt-flow from cracks to pores. It decreases when crack porosity decreases. The second important result from Figure 4c is a difference between dry LF and drained LF moduli, principally for moderate confining pressure. From a poroelastic theoretical point of view, these moduli should be equal. The difference could be explained by a rock-fluid physico-chemical interaction. This effect may be due to a coupling between the water and the crystals, probably feldspar microliths: processes of chemisorption at cracks surfaces can reduce surface energy, hence stiffness [*Baud et al.*, 2000].

[15] Two distinct effects have been indicated. One is a frequency effect and the other a physico-chemical effect. Both depend on the rock microstructure, and particularly on the interactions between cracks, pores and water. Our experimental data are applicable to the three first kilometers depth of the field scale (0–100 MPa of effective pressure), i.e., in the brittle upper part of the crust. They imply that - in that depth range - fluid and frequency effects have to be accounted for, if laboratory data are to be extrapolated at field scale.

[16] **Acknowledgments.** We would like to thank Ian Jackson and the anonymous reviewer for their constructive comments that helped to improve this paper. This work has been supported by Geoflux-Pays de la Loire and by 3F project SIMULAB of INSU.

References

Adam, L., and M. Batzle (2008), Elastic properties of carbonates from laboratory measurements at seismic and ultrasonic frequencies, *Leading Edge*, *27*, 1026–1032; doi:10.1190/1.2967556.

Adam, L., M. Batzle, and I. Brevik (2006), Gassman fluid substitution and shear modulus variability in carbonates at laboratory seismic and ultrasonic frequencies, *Geophysics*, *71*, F173, doi:10.1190/1.2358494.

Bala, M., and A. Cichy (2007), Comparison of p- and s-waves velocities estimated from Biot-Gassmann and Kuster-Toksoz models with results obtained from acoustic wavetrains interpretation, *Acta Geophys.*, *55*, 222–230.

Batzle, M., D. Han, and R. Hofmann (2006), Fluid mobility and frequency-dependent seismic velocity: Direct measurements, *Geophysics*, *71*, N1–N9, doi:10.1190/1.2159053.

Baud, P., W. Zhu, and T. Wong (2000), Failure mode and weakening effect of water on sandstone, *J. Geophys. Res.*, *105*, 19,371–19,390.

Biot, M. (1956), Theory of propagation of elastic waves in a fluid saturated porous solid. 2, Higher frequency range, *J. Acoust. Soc. Am.*, *28*, 168–178.

Cleary, M. (1978), Elastic and dynamic response regimes of fluid-impregnated solids with diverse microstructures, *Int. J. Solids Struct.*, *14*, 795–819.

Dunn, K. (1987), Sample boundary effect in acoustic attenuation of fluid-saturated porous cylinders, *J. Acoust. Soc. Am.*, *81*, 1259–1266.

Endres, A., and R. Knight (1997), Incorporating pore geometry and fluid pressure communication into modeling the elastic behavior of porous rock, *Geophysics*, *62*, 106–117.

Fortin, J., and Y. Guéguen (2007), Effects of pore collapse and grain crushing on ultrasonic velocities and $\frac{V_P}{V_S}$, *J. Geophys. Res.*, *112*, B08207, doi:10.1029/2005JB004005.

Fortin, J., A. Schubnel, and Y. Guéguen (2005), Elastic wave velocities and permeability evolution during compaction of Bleurswiller sandstone, *Rock Mech. Rock Eng.*, *42*, 873–889.

Gassmann, F. (1951), Uber die elasticizat poroser Medien, *Vierteljahrsschr. Naturforsch. Ges. Zuerich*, *96*, 1–23.

Geoffroy, L., and C. Dorbath (2008), Deep downward fluid percolation driven by localized crust dilatation in Iceland, *Geophys. Res. Lett.*, *35*, L17302, doi:10.1029/2008GL034514.

Guéguen, Y., and A. Schubnel (2003), Elastic wave velocities and permeability of cracked rocks, *Tectonophysics*, *370*, 163–176.

Le Ravalec, M., and Y. Guéguen (1996), High- and low- frequency elastic moduli for a saturated porous/cracked rock: Differential self-consistent and poroelastic theories, *Geophysics*, *61*, 1080–1094.

Mavko, G., and A. Nur (1975), Melt squirt in asthenosphere, *J. Geophys. Res.*, *80*, 1444–1448.

Nur, A., and G. Simmons (1969), The effect of saturation on velocity in low porosity rocks, *Earth Planet. Sci. Lett.*, *7*, 183–193.

O'Connell, R., and B. Budiansky (1974), Seismic velocities in dry and saturated cracked solids, *J. Geophys. Res.*, *79*, 5412–5426.

Schubnel, A., and Y. Guéguen (2003), Dispersion and anisotropy of elastic waves in cracked rocks, *J. Geophys. Res.*, *108*(B2), 2101, doi:10.1029/2002JB001824.

Schubnel, A., P. M. Benson, B. D. Thompson, J. F. Hazzard, and R. P. Young (2006), Quantifying damage, saturation and anisotropy in cracked rocks by inverting elastic wave velocities, *Pure Appl. Geophys.*, *163*, 947–973.

Sigurdsson, O., A. Gudmundsson, G. O. Fridleifsson, H. Franzon, S. P. Gudlaugsson, and V. Stefansson (2000), Database on igneous rock properties in Icelandic geothermal systems: Status and unexpected results, paper presented at World Geothermal Congress, Int. Geotherm. Assoc., Tohoku, Japan.

Stanchits, S., S. Vinciguerra, and G. Dresen (2006), Ultrasonic velocities, acoustic emission characteristics and crack damage of basalte and granite, *Pure Appl. Geophys.*, *163*, 1–20.

Tsuji, T., and G. Iturrino (2008), Velocity-porosity relationships in oceanic basalt from eastern flank of the Juan de Fuca Ridge: The effect of crack closure on seismic velocity, *Explor. Geophys.*, *39*, 41–51.

Wang, Z., and A. Nur (1990), Wave velocities in hydro-carbon saturated rocks: Experimental results, *Geophysics*, *55*, 723–733.

Wang, Z., M. Batzle, and A. Nur (1990), Effect of different pore fluids on seismic velocities in rocks, *Can. J. Explor. Geophys.*, *26*, 104–112.

M. Adelinet, J. Fortin, Y. Guéguen, and A. Schubnel, Laboratoire de Géologie, Ecole normale supérieure, 24 rue Lhomond, F-75005 Paris, France. (adelinet@geologie.ens.fr)

L. Geoffroy, LGRMP, UMR 6112, Université du Maine, CNRS, avenue Olivier Messiaen, F-72085 Le Mans, France.